# Low-temperature kinetics of exciton–exciton annihilation of weakly localized one-dimensional Frenkel excitons

Ryzhov, I. V.; Kozlov, G. G.; Malyshev, V. A.; Knoester, J.

*Published in:*
Journal of Chemical Physics

*DOI:*
10.1063/1.1352080

# Low-temperature kinetics of exciton–exciton annihilation of weakly localized one-dimensional Frenkel excitons

I. V. Ryzhov
*Herzen Pedagogical University, Moika 48, 191186 Saint-Petersburg, Russia*

G. G. Kozlov and V. A. Malyshev
*National Research Center, ''Vavilov State Optical Institute,'' Birzhevaya Liniya 12, 199034 Saint-Petersburg, Russia*

J. Knoester
*Institute for Theoretical Physics and Material Science Center, University of Groningen, Nijenborgh 4, 9747 AG Groningen, The Netherlands*

(Received 30 October 2000; accepted 10 January 2001)

We present results of numerical simulations of the kinetics of exciton–exciton annihilation of weakly localized one-dimensional Frenkel excitons at low temperatures. We find that the kinetics is represented by two well-distinguished components: a fast short-time decay and a very slow long-time tail. The former arises from excitons that initially reside in states belonging to the same localization segment of the chain, while the slow component is caused by excitons created on different localization segments. We show that the usual bimolecular theory fails in the description of the behavior found. We also present a qualitative analytical explanation of the nonexponential behavior observed in both the short- and the long-time decay components. Finally, it is shown that our theoretical estimate for the annihilation time of the fast component is in good agreement with data obtained from transient absorption experiments on *J*-aggregates of pseudoisocyanine. © *2001 American Institute of Physics.* [DOI: 10.1063/1.1352080]

## I. INTRODUCTION

Exciton–exciton annihilation is an important process that strongly influences the optical and optoelectronic properties of materials at high excitation densities. In particular, exciton–exciton annihilation affects the nonlinear and lasing properties of organic systems, such as *J*-aggregates and polymer films.[1] Though the importance of this process is well-recognized, the microscopic understanding of the annihilation kinetics is still rather poor. This holds especially under the conditions of strong exciton delocalization and (or) low temperature, where the usual bimolecular theory of exciton–exciton annihilation is expected to break down. The aim of this paper is to study the annihilation kinetics in weakly disordered one-dimensional Frenkel exciton systems, where the exciton coherence size can be considerable (tens of lattice units). This study is of relevance to the optical properties and exciton dynamics in *J*-aggregates and molecular antenna systems.

The standard approach to describe the kinetics of exciton–exciton annihilation relies on the bimolecular rate equation, in which it is assumed that the effective annihilation rate is proportional to the exciton density. This equation reads[2–6]

$$\dot{n} = -\gamma n - \alpha n^2, \tag{1}$$

where $n$ represents the average exciton density, understood here as the number of excitations per molecule, $\gamma$ is the single-excitation (radiative and nonradiative) relaxation rate, and $\alpha$ is the co-called annihilation constant having here the dimension of 1/time. The effective rate of exciton–exciton annihilation in the system is then indeed proportional to the average exciton density $n$ and is given by $\alpha n$. The solution to Eq. (1) reads

$$n = \frac{\gamma n_0}{\gamma e^{\gamma t} + \alpha n_0 (e^{\gamma t} - 1)}, \tag{2}$$

where $n_0$ is the initial population of excitations. If the annihilation dominates the single-exciton relaxation ($\alpha n_0 \gg \gamma$) the excitation population decreases according to a hyperbolic (nonexponential) law,

$$n = \frac{n_0}{1 + \alpha n_0 t}. \tag{3}$$

The typical picture that one commonly has in mind when modeling the annihilation process as is done in Eq. (1), is as follows. First, it is usually understood that, as a result of strong disorder and (or) high temperature, the Frenkel excitons represent, in fact, molecular excitations.[2–6] Next, it is assumed that the excitations (diffusively) move over the system. If the diffusion rate is large compared to the rate of nearest-neighbor annihilation, denoted by $w_0$, two excitations annihilate each other (by fusing into one high-lying molecular excitation that quickly loses its energy by vibrational relaxation) when they have reached neighboring molecules. In this case $\alpha = w_0$. On the other hand, if $w_0$ dominates the diffusion rate, the annihilation event may occur at a distance large compared to the the nearest-neighbor separation. In this case, the annihilation constant is determined by a

 

convolution of the annihilation rate with the pair correlation function of two excitations,[7] and may in principle depend on time.

The bimolecular rate description has limitations, which become rather important at low temperatures. Obviously, the bimolecular approach does not account for the fact that the excitons in *J*-aggregates are generally quite strongly spread, with typical coherence lengths of several tens of molecules.[8–14] Even at room temperature, this length is of the order of 10 molecules,[15–17] owing to the large intermolecular excitation transfer interaction in these systems. It is an open and interesting question whether this finite length may be accounted for by interpreting $\alpha$ in Eq. (1) as an effective annihilation constant. In this paper, we will address this question for low-temperature exciton systems.

We will study the kinetics of exciton–exciton annihilation of one-dimensional excitons that are weakly localized by static disorder. We will use the same framework as was done in Refs. 18 and 19 to calculate annihilation rates. The new element of the present paper is to use these rates to follow the kinetics of annihilation. An important step in describing the annihilation of extended excitons, is to distinguish between inter- and intrasegment annihilation.[18,19] The rationale for this distinction is as follows. As appears from numerical simulations of disordered exciton chains, the exciton states residing close to the bottom of the exciton band (the region that dominates the optical response) can be classified into groups of a few (two or three) states. The states within each separate group are all localized on the same segment of the aggregate, with a typical size $N^*$ (often referred to as the number of coherently bound molecules), while the segments corresponding to different groups do not overlap. In fact, it turns out that the two or three exciton states within each such group are very similar in structure and energy to the lowest two or three states that exists on an ordered chain of length $N^*$.[20–23] In particular, the lowest state of such a group has a wave function spread over the segment without nodes and can be interpreted as the local ground state. The next higher lying state of the group has a well-defined node and looks like a first local excited state, etc. The energy difference of the local ground and first excited states agrees well with that of a perfect chain of length $N^*$.

Obviously, to describe exciton–exciton annihilation, one should consider at least the two-exciton states. As is well known, one-dimensional Frenkel excitons are weakly interacting fermions (see Refs. 24–28). Thus, the wave functions of states with two excitons can be composed of Slater determinants of two one-exciton wave functions. Under the condition of weak localization, two different types of two-exciton states then appear: (i) those with two excitons belonging to the same localization segment, and (ii) those with the two excitons localized on different segments. This immediately leads to the distinction of intrasegment and intersegment annihilation as fundamentally different annihilation channel.[18,19]

This paper is organized as follows: In Sec. II, we present our microscopic model of annihilation, express the annihilation rate in terms of the basic interactions and wave functions, and make the formal step towards the annihilation kinetics at low temperatures, where the diffusive motion of excitons towards each other may be neglected. In Sec. III we use the distinction between inter- and intrasegment annihilation to derive qualitatively analytical expressions for the low-temperature annihilation kinetics. A more detailed study is presented in Sec. IV, where we basically exactly solve the kinetics, formally defined in Sec. II, through numerical simulations. In Sec. V we summarize our findings and discuss the relevance to experimental low-temperature annihilation data.

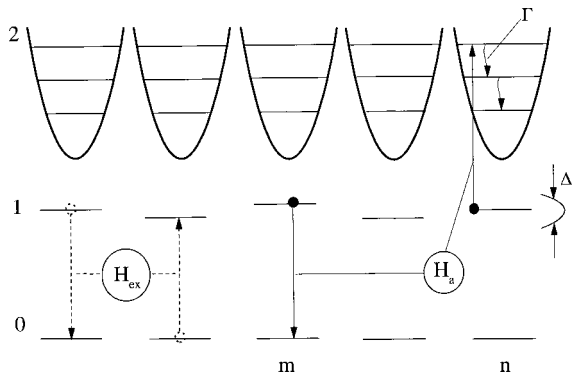


FIG. 1. Schematic representation of all interactions contributing to the exciton–exciton annihilation process. The interaction $H_{ex}$, indicated by the dashed lines, forms excitonic states in the subspace of the molecular states ''0'' and ''1.'' Excitons annihilate through a high-lying electronic-vibrational molecular term ''2'' ($\omega_{10} \approx \omega_{21}$). The first step of the annihilation process results from the intermolecular interaction $H_a$, which induces simultaneous transitions of the molecule $m$ to the ground state and molecule $n$ to the high-lying term. The second step results from fast vibrational relaxation within high-lying electronic-vibrational sublevels towards the ground vibrational state characterized by a rate $\Gamma \gg H_a$.

## II. TWO-EXCITON ANNIHILATION MODEL

### A. Motivation

Under usual experimental conditions, only a small part of the localization segments on molecular aggregates are excited. For example, the authors of Refs. 12 and 14 estimated that in their experiments, one hundred molecules per aggregate were produced at the highest excitation power applied ($0.98\,\mathrm{GW/cm^2}$). As a physical aggregate normally consists of $\sim 10^4$ molecules,[3,5] while the typical localization segment in their particular case counted 20 molecules, these authors concluded that less than one exciton was created per segment of localization (on average, one exciton per five segments). A simple consideration based on the Poisson distribution for the probability of finding an integer number of excitons per segment, shows that on the physical aggregate about 80 out of 500 segments are expected to be singly excited, while only 8 are doubly excited. Triply (and more) excited segments are almost absent. Bearing in mind that excitons, created on the same segment of an aggregate or on closely spaced separate segments, will annihilate first, we conclude that a two-exciton model of annihilation seems to be quite reasonable as a first step.

### B. Rate of two-exciton annihilation

As a working model, we adopt a linear chain of $\mathcal{N}$ three-level molecules as depicted in Fig. 1.[2,18,19] The two lower

molecular states, denoted ''0'' and ''1,'' are assumed to form an exciton band, as a result of a sufficiently strong resonant dipole–dipole intermolecular coupling. The corresponding exciton Hamiltonian, taken in the nearest-neighbor approximation, reads

$$H_{\mathrm{ex}}=-U\sum_{n=1}^{\mathcal{N}-1}(b_{1n}^{+}b_{1,n+1}+b_{1,n+1}^{+}b_{1n})+\sum_{n=1}^{\mathcal{N}}E_{1n}b_{1n}^{+}b_{1n}, \tag{4}$$

where $-U<0$ is the nearest-neighbor hopping integral chosen to be negative, as is the case for $J$-aggregates, and $b_{1n}^{+}(b_{1n})$ denotes the Pauli creation (annihilation) operator of the first excited state of molecule $n$ (the state with all the molecules in their ground states serves as the vacuum state $|0\rangle$ and has zero energy). The second term in Eq. (4) represents the Hamiltonian of noninteracting molecules, in which $E_{1n}=E_1+\Delta_n$ is the energy of the first excited state of molecule $n$ with $E_1$ and $\Delta_n$ being, respectively, the mean value of the energy and a static random offset. The latter simulates on-site (diagonal) disorder and results in localization of the excitonic states. Fluctuations of the nearest-neighbor coupling are neglected. It will be assumed that $\Delta_n$ is distributed uniformly within the interval $[-\Delta,\Delta]$, so that the typical magnitude of the disorder is given by the standard deviation $\sigma=\Delta/\sqrt{3}$. For $\sigma\ll U$ the exciton eigenfunctions are localized within rather large segments of the chain, $1\ll N^{*}\ll\mathcal{N}$.[20–23,29,30] Throughout this paper, we will assume that this condition holds.

The high-lying electronic-vibrational molecular term, depicted as ''2'' in Fig. 1, serves as the intermediate state through which annihilation occurs.[2,18,19] We consider one of the electronic-vibrational levels to be resonant with the two-exciton optical states and to undergo an efficient phonon-assisted relaxation to the ground vibronic state (see Fig. 1). The annihilation process itself consists of transferring the energy of two excitons to the high-lying molecular term. Assuming this step to occur due to the resonant dipole–dipole intermolecular interaction, we may write the corresponding Hamiltonian as follows:

$$H_a=\frac{1}{2}\sum_{m,n=1}^{\mathcal{N}}\frac{V}{|n-m|^3}b_{1n}b_{1m}(b_{2n}^{+}+b_{2m}^{+})+\mathrm{h.c.}, \tag{5}$$

where $V$ is the matrix element of the annihilation operator for nearest neighbors and $b_{2n}^{+}(b_{2n})$ denotes the Pauli creation (annihilation) operator of the high-lying state of molecule $n$. The operator (5) annihilates the two excitations occupying molecules $m$ and $n$ and excites one of these molecules in the high-lying state. The implication of $H_a$ for third-order nonlinear optics of $J$-aggregates has been studied in Ref. 31.

In accordance with our arguments in Sec. II A, we will assume that not more than two excitons are created by the pump per linear chain. Moreover, we will assume that $|V|$ is small compared to the rate, $\Gamma$, of phonon-assisted relaxation in the high-lying molecular state. We may then use perturbation theory to calculate the rate of annihilation. Moreover, the back process (exciton fission) can then be neglected. The resulting expression for the rate of exciton–exciton annihilation starting from the two exciton eigenstate $|\mu\nu\rangle$ $(1\leqslant\mu<\nu\leqslant\mathcal{N})$ is simply given by the ''Golden Rule,''

$$w_a^{\mu\nu}=\frac{2\pi}{\hbar}\rho(E_f)\sum_{n=1}^{\mathcal{N}}|\langle 2n|H_a|\mu\nu\rangle|^2, \tag{6}$$

where $\rho(E_f)$ is the density of final states (hereafter replaced by $1/\Gamma$). Because of the fermionic nature of one-dimensional Frenkel excitons, one can compose the two-exciton eigenfunctions as Slater determinants of the one-exciton eigenfunctions,

$$|\mu\nu\rangle=\sum_{m=1}^{\mathcal{N}}\sum_{n<m}^{\mathcal{N}}\psi_{\mu m;\nu n}|1m,1n\rangle, \tag{7a}$$

$$\psi_{\mu m;\nu n}=\varphi_{\mu m}\varphi_{\nu n}-\varphi_{\mu n}\varphi_{\nu m}, \tag{7b}$$

where $\{\varphi_{\nu n}\}$ are the eigenfunctions of the one-exciton problem,

$$\sum_{m=1}^{\mathcal{N}}H_{ex}^{nm}\varphi_{\nu m}=E_{\nu}\varphi_{\nu n}. \tag{8}$$

Here, $H_{\mathrm{ex}}^{nm}=\langle 1n|H_{\mathrm{ex}}|1m\rangle$ and $E_{\nu}$ is the eigenenergy of the one-exciton state $\nu$. Substituting Eq. (7b) into Eq. (6) one obtains[19]

$$w_a^{\mu\nu}=\frac{2\pi V^2}{\hbar\Gamma}\sum_{m=1}^{\mathcal{N}}\left[\sum_{n=1}^{\mathcal{N}}{}'\frac{\psi_{\mu m;\nu n}}{(m-n)^3}\right]^2, \tag{9}$$

where the prime denotes that $n\neq m$. In particular, for a dimer $(\mathcal{N}=2)$ only one two-exciton state exists and its annihilation rate is given by

$$w_a^{12}=w_0=\frac{4\pi V^2}{\hbar\Gamma}. \tag{10}$$

In order to arrive at Eq. (9) we used the fact that Frenkel excitons are noninteracting fermions whenever the nearest-neighbor approximation is used for the hopping integrals. They become interacting quasiparticles when including the coupling to far neighbors. The importance of the latter can be estimated through the changes which the long-range terms produce in the density of exciton states. It is known that in one-dimensional aggregates, the long-range dipole–dipole interactions shift the exciton band bottom by approximately 20% compared to the nearest-neighbor model.[21,29] The smallness of this shift suggests the corrections due to long-range interactions to be of a perturbative nature. Indeed, for few-particle states, Frenkel excitons are weakly interacting (well-defined) fermions, despite the long-range coupling.

Furthermore, as follows from the results of both numerical simulations[29] and theoretical estimates[21] of the linear optical properties of disordered Frenkel chains, the oscillator strengths of the optical transitions near the lower band edge grow by approximately a factor of 2.5 due to the long-range dipole–dipole interactions. This results from a larger extension of the optically active exciton states in the exact dipole–dipole model compared to the nearest-neighbor model (at a fixed disorder strength). In principle, this effect is not of a perturbative nature. It can, however, be included into the final formulas for the annihilation rates (see below) by res-

caling the number of coherently bound molecules $N^*$. The above arguments justify the nearest-neighbor framework as a reasonable approach to describe Frenkel excitons.

It is worth stressing, though, that the dipole–dipole interaction in the annihilation channel ($H_a$) can generally not be taken in the nearest-neighbor approximation, because the annihilation of two excitons localized on separate localization segments is determined by the coupling to far neighbors.

### C. Low-temperature annihilation kinetics

As in the present paper we are mainly interested in the annihilation kinetics itself, we will neglect any other possible channel of population relaxation, such as the radiative transitions from two-exciton to one-exciton states (also acting towards lowering the exciton population), as well as a possible multiphonon relaxation from the high-lying term to the one-exciton states (acting, on the contrary, towards raising again the exciton population). To calculate the kinetics of the exciton–exciton annihilation, we will assume that excitons are created by a resonant laser pulse, that is short compared to the inverse of the $J$-band width. Under these conditions, the initial populations of the two-exciton state $|\mu\nu\rangle$ is proportional to the corresponding oscillator strength $F_{\mu\nu}$ given by

$$F_{\mu\nu}=|\langle\mu\nu|D^2|0\rangle|^2=\left(\sum_{m,n=1}^{\mathcal{N}}\psi_{\mu m;\nu n}\right)^2, \tag{11}$$

where $D=\Sigma_{n=1}^{N}(b_{1n}^{+}+b_{1n})$ is the chain's dipole operator (the chain length is assumed to be smaller than the emission wavelength).

After the initial creation process, excitons may in principle move over the chain, At low temperature, however, the possibility to move is very restricted and the optically excited localized Frenkel excitons are practically immobile.[18] The reason is that at low temperature ($T\leqslant$ width of $J$-band), an exciton created in one of the local ground states may move to an other similar state only when the latter has an energy lower than the former. The typical energy offset between the local ground states is of the order of the width of their energy distribution (i.e., the width of the $J$-band). Therefore, after one jump the exciton typically resides in the tail of this distribution. The number of states with still lower energy then drastically reduces, giving rise to a strong increase of the mean distance to such lower energy states. In fact, already after one jump the exciton has a strongly suppressed chance to jump further, i.e., such a type of the spatioenergetic diffusion (towards lowering the energy) is stopped rapidly and does not yield a sufficient possibility for two excitons to approach each other and annihilate. It is worth noting that experiments also indicate the absence of such a diffusion, which would manifest itself in a redshift of the exciton emission spectrum relative to the absorption spectrum. The experimental data show that such a Stokes shift is either absent or has a small magnitude.[8,9,13] A similar situation occurs in glasses doped with rare-earth ions.[32]

Following the above arguments, we will assume that two excitons annihilate from the positions where they have been created. Then, the time dependence of the population of the excited two-exciton states is given by

$$P_a(t)=2\left\langle\sum_{\mu\nu}f_{\mu\nu}\exp(-w_a^{\mu\nu}t)\right\rangle, \tag{12}$$

where $f_{\mu\nu}=F_{\mu\nu}/\Sigma_{\mu\nu}F_{\mu\nu}$ and angular brackets denote an average over the disorder realizations. Note that we have normalized the population such that it equals 2 at $t=0$. Formula (12) will be the basis of our further analysis of the low-temperature annihilation kinetics.

## III. QUALITATIVE PICTURE

Before carrying out numerical simulations, we first provide a qualitative analysis of Eq. (12). Following the arguments concerning the nature of the low-energy weakly localized one-dimensional states, we separate the summation in Eq. (12) into two parts: $P_a(t)=P_a^{\text{intra}}(t)+P_a^{\text{inter}}(t)$. The first part, $P_a^{\text{intra}}(t)$, includes all those terms $\{\mu\nu\}$, where the one-exciton states $\mu$ and $\nu$ are localized on the same chain segment (doubly excited segments). The second part, $P_a^{\text{inter}}(t)$, contains those terms where $\mu$ and $\nu$ reside on different segments. The fact that this distinction can only be made for low-energy states is no restriction, as anyhow these states are the ones that dominate the ground state to one-exciton and the one-to-two-exciton absorption spectrum. Using the picture of exciton states on a chain of effective length $N^*$, one arrives at the intrasegment annihilation rate,[18,19]

$$w_a^{\text{intra}}=\frac{5\pi^6}{18(N^*+1)^3}w_0, \tag{13}$$

where $w_0$ is given by Eq. (10) and the factor $5\pi^6/18\approx 270$.

The second term, $P_a^{\text{inter}}(t)$, governs the annihilation of two excitons created on different localization segments and is characterized by the rate[19]

$$w_a^{\text{inter}}=\frac{N^*+1}{R^6}w_0, \tag{14}$$

where $R$ is the distance between the two excited segments. Note that the rate of the intersegment annihilation scales linearly with $N^*+1$. As the wave functions of both segments enter the expression for $w_a^{\text{inter}}$, one might intuitively expect a quadratic dependence on $N^*+1$. However, only one of the two excited segments, namely the one that passes to the ground state $|0\rangle$ in the annihilation process, coherently contributes to $w_a^{\text{inter}}$ giving the factor $N^*+1$ (so-called superradiant transition). The transition within the other excited segment occurs to the high-lying molecular state of each molecule. It is important to note that the latter events are summed incoherently, as is evident from Eq. (9), thus preventing the appearance of an extra power of $N^*+1$.

Keeping in mind that $R\geqslant N^*$ as well as that the numerical factor in Eq. (13) is fairly large, one immediately deduces from Eqs. (13) and (14) that $w_a^{\text{intra}}\gg w_a^{\text{inter}}$ provided that $N^*$ is of the order of or larger than several units, which is the condition we will focus on in the simulations. From this, one expects that the kinetics of the exciton–exciton annihilation will consist of two distinct parts: a very fast short-time de-

cay, described by $P_a^{\text{intra}}(t)$, and a very slow long-time tail for which $P_a^{\text{inter}}(t)$ is responsible. In order to estimate the relative weight of these two components, we will take into account the fact that the oscillator strengths of double excitation of a particular localization segment and excitation of two different segments are of the same order. Then, statistical arguments based on the Poisson distribution seem to be sufficient for making estimates. If the initial density of excitations equals $n_0$ (in our case, $n_0=2/\mathcal{N}$), the probability of finding a typical localization segment (of length $N^*$) to be $k$-fold excited reads

$$p(k)=\frac{(n_0N^*)^k}{k!}e^{-n_0N^*}. \tag{15}$$

Therefore, the probabilities of double excitation of a typical localization segment and of excitation of two different segments are given by $0.5(n_0N^*)^2e^{-n_0N^*}$ and $2n_0N^*e^{-n_0N^*}$, respectively. Thus, the relative contribution of the shorter component in $P_a(t)$ is of the order of $0.25n_0N^*$, which drops upon increasing the disorder strength $\sigma$ (or upon a corresponding decrease of $N^*$) and grows with increasing the density of excitations $n_0$.

Now, we turn to a discussion of the character of the annihilation kinetics. We recall that in the bimolecular model, the decay is nonexponential, as a result of the nonlinearity of the driving equation (1). We will argue that in our case, the kinetics is also nonexponential, which, however, does not result from a nonlinearity. Let us consider first the intrasegment channel of annihilation. Here, according to Eq. (12), the nonexponentiality is expected even in the absence of disorder (i.e., for a regular chain), because the annihilation rate $w_a^{\mu\nu}$ obviously depends on which exciton states are involved in the annihilation process (see Sec. IV). In the presence of disorder, there is an additional source for the nonexponential behavior of annihilation through the intrasegment channel. It originates from the fluctuations in the sizes of the localization segments, $N$. Equation (13) gives the typical magnitude of the intrasegment annihilation rate. In reality, $N^*$ in Eq. (13) should be replaced by a fluctuating value $N$. Consequently, the sum over the overlapping states in Eq. (12) can be approximately substituted by an average over a distribution of $N$, $G(N)$. One then obtains

$$P_a^{\text{intra}}(t)\approx 2\int dNG(N)\exp[-w_a^{\text{intra}}(N)t]. \tag{16}$$

As follows from numerical simulations,[21,22,29,33] the standard deviation of $N$, $[\int dNG(N)(N-\bar{N})^2]^{1/2}$, is of the order of the mean, $\bar{N}=\int dNG(N)N$, i.e., the distribution $G(N)$ is rather broad. Due to this fact, the resulting nonexponentiality is expected to be considerable. The numerical simulations presented in Sec. IV confirm this picture.

The origin of the nonexponential behavior of the intersegment annihilation is twofold. First, the corresponding annihilation rate, as in the previous case, depends on the size of the localization segment $N$ [see Eq. (14)]. Thus, fluctuations of the latter will affect the annihilation kinetics even for a fixed distance between excited segments. However, the character of the intersegment annihilation is determined mostly by the strong dependence of the annihilation rate (14) on the distance between two excited segments, $R$. The annihilation kinetics caused by the fluctuations of $R$ is simply given by an average of the pair kinetics $2\exp[-w_a^{\text{inter}}(R)t]$ over all realizations of $R$. In order to obtain an analytical estimate, let us assume that the density of excited segments is low (as is in our case), so that $R$ can be treated as a continuous stochastic variable. Then the annihilation kinetics is given by an integral similar to that in Eq. (16) with $G(N)$ replaced by a suitable $R$-distribution function, $G(R)$. We will adopt a uniform distribution for $R$, $G(R)=N^*/\mathcal{N}$, assuming that the probability of finding a segment to be excited is equal to the inverse of the number of segments in the chain, $\mathcal{N}/N^*$. In evaluating the integral, we will extend the integration over the entire positive axes, neglecting thus the minimal distance between two adjacent segments as well as the finiteness of the chain. Both approximations are justified at a low density of excitations. One thus arrives at

$$\begin{aligned}P_a^{\text{intra}}(t)&\approx 2\left[1-\frac{N^*}{\mathcal{N}}\int_0^\infty dR(1-e^{-w_a^{\text{inter}}(R)t})\right]\\&\approx 2\left[1-\Gamma\left(\frac{5}{6}\right)\frac{N^*}{\mathcal{N}}(N+1)^{1/6}(w_0t)^{1/6}\right],\end{aligned} \tag{17}$$

where $\Gamma(x)$ is the Gamma-function. Equation (17) is correct provided that the second term on the right-hand side is less than unity. This holds in a very large time interval, determined by the inequality $\Gamma(5/6)N^*(N+1)^{1/6}(w_0t)^{1/6}<\mathcal{N}$. It follows from the stretched exponential behavior of Eq. (17) that further averaging of $P_a^{\text{intra}}(t)$ over the $N$-distribution will not change the character of the kinetics and results, in fact, in replacing $N$ by $N^*$.

To conclude this section, we note that the (''artificial'') quantity $P_a(t)$ can be simply rescaled to the measurable magnitude—the density of excitons $n(t)=P_a(t)/\mathcal{N}$. Introducing the initial exciton density $n_0=2/\mathcal{N}$, we obtain

$$n^{\text{intra}}(t)\approx n_0\left[1-\frac{1}{2}\Gamma\left(\frac{5}{6}\right)n_0N^*(N^*+1)^{1/6}(w_0t)^{1/6}\right]. \tag{18}$$

## IV. NUMERICAL SIMULATIONS AND DISCUSSION

To study the annihilation kinetics in more detail, we have carried out numerical simulations for a chain of length $\mathcal{N}=200$. For such a length, the mean initial density of excitations is $n_0=0.01$. We calculated the one-exciton eigenfunctions $\varphi_{\nu n}$ by diagonalizing numerically the Frenkel Hamiltonian (4) for a particular realization of disorder, and then composed two-exciton eigenfunctions according to Eq. (7). Using further Eq. (9) and Eq. (11), we computed the rate of annihilation, $w_a^{\mu\nu}$, and the oscillator strength, $F_{\mu\nu}$, for any two-exciton state $|\mu\nu\rangle$. Then Eq. (12) was used to evaluate the annihilation kinetics. The resulting kinetics was obtained by averaging over 20 realizations of disorder. An increase of this number did not lead to considerable changes in the calculated curves. As a time unit, we used $w_0^{-1}$. The results of the simulations for different values of $\Delta/U$ are depicted in Figs. 2–5 by thick solid lines.

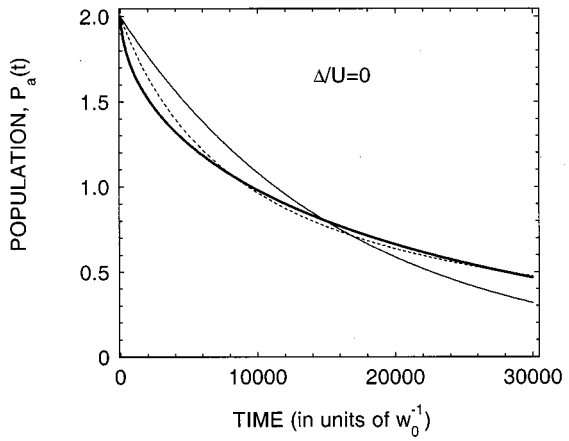


FIG. 2. Plot of the exciton–exciton annihilation kinetics obtained from numerical simulations for a regular linear chain of 200 sites (thick solid line). The least-square fits by means of the exponential $2\exp(-w_0t/a)$ with $a=1.63\cdot10^4$ as well as by the bimolecular model (3), taken in the form $2/(1+bw_0t)$ with $b=1.07\cdot10^{-4}$ are presented by the thin solid and dashed lines, respectively. The time unit is chosen to be $w_0^{-1}$ [see Eq. (10)].

Figure 2 represents the annihilation kinetics for a perfect chain ($\Delta=0$), as well as a least-square fit by means of an exponential $2\exp(-w_0t/a)$ (thin solid line), achieved at $a=1.63\cdot10^4$. The fit clearly demonstrates that the calculated curve cannot be matched by a single exponential. This unambiguously means that not only the states with $\mu=1$ and $\nu=2$, having the largest oscillator strengths, contribute to the sum in Eq. (12), but the other states contribute a comparable amount. The time scale of the kinetics depicted in Fig. 2 qualitatively corresponds to that calculated by using Eq. (13)

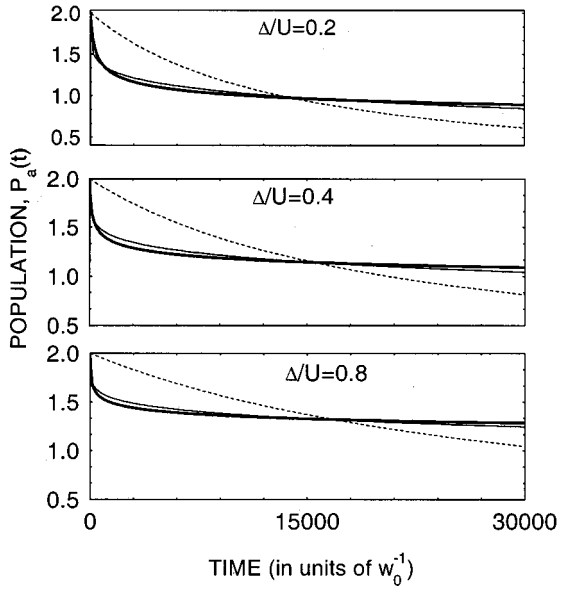


FIG. 3. Plots of the exciton–exciton annihilation kinetics obtained from numerical simulations (thick solid lines) for a linear chain of 200 sites at different values of the degree of disorder $\Delta/U$. Thin solid lines give the least-square fits by means of the function $2-ct^{1/6}$ at $c=0.21$ ($\Delta/U=0.2$), $c=0.17$ ($\Delta/U=0.4$), and $c=0.14$ ($\Delta/U=0.8$). Dashed lines give the best fit using the bimolecular model (3). The time unit is chosen to be $w_0^{-1}$.

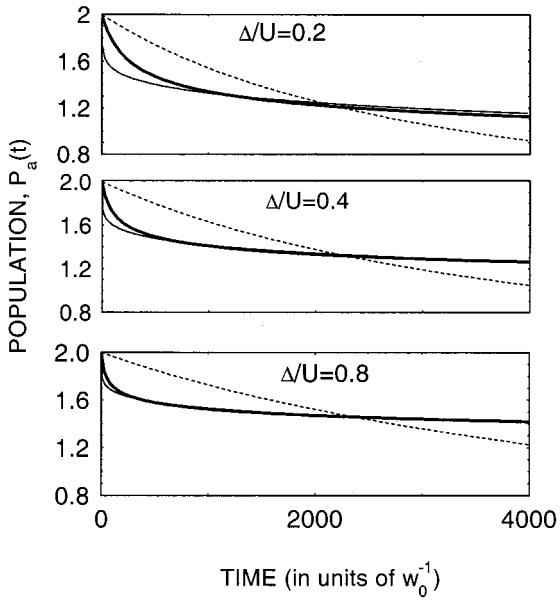


FIG. 4. As Fig. 3, but now focused on the initial stage of the annihilation process. For this time interval, the best fits by means of the function $2-ct^{1/6}$ were achieved at $c=0.21$ ($\Delta/U=0.2$), $c=0.18$ ($\Delta/U=0.4$), and $c=0.15$ ($\Delta/U=0.8$).

with $N^*$ replaced by $\mathcal{N}$: at $\mathcal{N}=200$, one obtains $w_a^{\text{intra}}\sim3\times10^{-5}w_0$.

We also tried to fit the numerical curve in Fig. 2 by means of the bimolecular equation (3) taken in the form $2/(1+bw_0t)$. The best fit was achieved at $b=1.07\cdot10^{-4}$ and is plotted in Fig. 2 by the dashed line. At first glance, it seems that the latter almost matches the numerical data except, maybe, at the initial stage. However, the fitting constant $b$, carrying, in fact, the meaning of the density of excitations (see the discussion presented in the Introduction), underestimates the real value $n_0=0.01$ by two orders of magnitude.

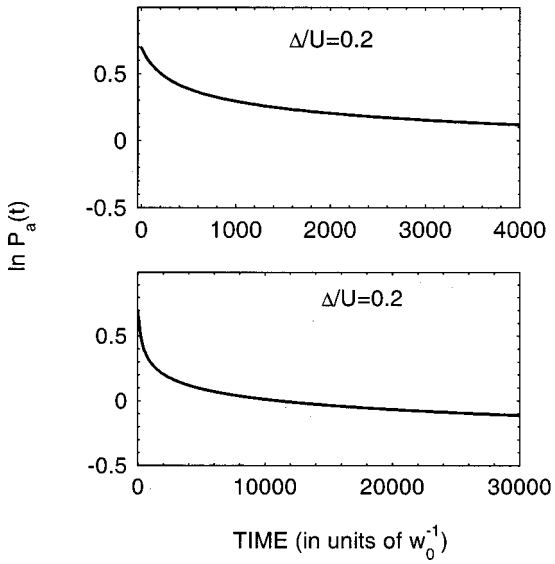


FIG. 5. Log-plot of the exciton–exciton annihilation kinetics for a linear chain of 200 sites at $\Delta/U=0.2$, demonstrating the nonexponential character of the decay. The time unit is chosen to be $w_0^{-1}$.

Figures 3 and 4 show the numerical results obtained for disordered chains with different degrees of disorder, $\Delta/U$. In Fig. 3, we plotted the annihilation decay curves in a wide time interval, while Fig. 4 presents the initial stages of the annihilation process. From the numerical results presented in Figs. 3 and 4 several conclusions can be deduced. First of all, it is clearly seen that the entire kinetics indeed consists of two well-distinguished components: a fast short-time decay, becoming faster as the disorder is increased, and a very slow long-time tail. The weight of the faster component is smaller than that for the slower one and drops upon increasing the disorder strength $\Delta/U$.

It is reasonable to relate these two components to the intra- and intersegment channels of exciton–exciton annihilation, respectively, in accordance with the qualitative picture discussed in the previous section. Indeed, let us use for the typical size $N^*$ of a localization segment the well-known estimate[20,21,29,30]

$$N^*+1=\left(3\pi^2\frac{U}{\sigma}\right)^{2/3}. \tag{19}$$

Recall that in our case $\sigma=\Delta/\sqrt{3}$. Substituting Eq. (19) into Eq. (13), one gets

$$w_a^{\mathrm{intra}}=\frac{5\pi^2}{506}\left(\frac{\Delta}{U}\right)^2 w_0\approx 0.1\left(\frac{\Delta}{U}\right)^2 w_0. \tag{20}$$

Equation (20) gives us the disorder scaling of the intrasegment annihilation rate. Accordingly, we arrive at the following estimates: $w_a^{\mathrm{intra}}\sim 4\times10^{-3}w_0$, $2\times10^{-2}w_0$, and $6\times10^{-2}w_0$, respectively for $\Delta/U=0.2$, 0.4, and 0.8. Indeed, these numbers qualitatively match the time scales of the fast components (see Fig. 4).

We also plotted in Figs. 3 and 4 the least square fits of the numerical data by means of the function $2-c(w_0t)^{1/6}$ (thin solid line). One observes that at higher degree of disorder ($\Delta/U=0.8$), when the weight of the faster component is smallest, the fitting function fairly well follows the numerical curve over almost the entire time interval of decay. The value of the fitting constant $c=0.14$–$0.15$ is of the same order as the one deduced from the theory, Eq. (17), according to which it must be $2\Gamma(5/6)(N^*)^{7/6}/\mathcal{N}=2\Gamma(5/6)\times(3\sqrt{3}\pi^2U/\Delta)^{7/9}/\mathcal{N}\approx 0.24$ [The discrepancy probably stems from neglecting $N^*$ as a minimal separation in Eq. (17).] This unambiguously means that the intersegment channel dominates the long-time part of the annihilation kinetics. It should be especially stressed that the bimolecular fits, shown in Figs. 3 and 4 by the dashed lines, fail absolutely in the description of the numerical data.

In order to show the character of the decay (exponential or nonexponential) in the case of disordered chains, we depicted in Fig. 5 the log-plot of the calculated annihilation kinetics for $\Delta/U=0.2$. As can be seen, neither of the two components shows an exponential behavior.

## V. SUMMARY AND CONCLUDING REMARKS

In this paper we have studied the low-temperature kinetics of exciton–exciton annihilation of weakly localized one-dimensional Frenkel excitons using a two-exciton static model (immobile quasiparticles) with diagonal disorder. Our analysis leads to three main conclusions:

(i) The entire kinetics consists of two well-distinguished components: a very slow long-time decay and a much faster short-time drop. The latter component becomes faster with higher degree of disorder. The weight of the faster component is much smaller than that of the slower one, and decreases with increasing disorder strength.
(ii) Neither of these two components shows an exponential behavior.
(iii) The usual bimolecular theory fails in the description of the behavior found.

These findings are well-understood from the existence of two competing options for two excitons to annihilate. The slower component is driven by the annihilation of exciton states localized on different segments of the chain, while the faster one originates from the annihilation of doubly excited segments. Fluctuations of distances between two excitons and sizes of the localization segments explain the nonexponential nature of the slower and faster components, respectively.

It is worthwhile to estimate the typical rates of both annihilation channels for existing $J$-aggregates. In order to do this, we need information concerning the parameters $U$, $V$, and $\Gamma$. For $J$-aggregates $U\sim1000\,\mathrm{cm}^{-1}$ is quite typical.[8,10,13,28] Less information consists concerning the annihilation interaction $V$, but as we assumed it to be of dipolar origin it seems not unreasonable to take a value similar to $U$. This is, in fact, supported by semi-empirical calculations of higher molecular singlet states of pseudoisocyanine (PIC) molecules.[34] These calculations indicate a molecular $S_1\rightarrow S_2$ transition that is similar in energy and oscillator strength as the $S_0\rightarrow S_1$ transition responsible for PIC's well-known $J$-band. We thus take $V\sim1000\,\mathrm{cm}^{-1}$. Finally, we will take $\Gamma\sim3000\,\mathrm{cm}^{-1}$, corresponding to a vibrational relaxation time in the $S_2$ state of about 10 fs. Using these numbers, we arrive at $w_a^{\mathrm{intra}}\sim3\times10^{16}N^{*-3}\,\mathrm{s}^{-1}$. The corresponding estimate for the inter-segment annihilation rate taken for adjacent segments ($R=N^*$) reads $w_a^{\mathrm{inter}}\sim10^{14}N^{*-5}\,\mathrm{s}^{-1}$.

At low temperatures, the quantity $N^*$ is found to be of the order of several tens.[8,10–13] Letting $N^*=20$, as was reported in Refs. 12 and 14, we arrive at $w_a^{\mathrm{intra}}\sim4\times10^{12}\,\mathrm{s}^{-1}$ and $w_a^{\mathrm{inter}}\sim3\times10^{7}\,\mathrm{s}^{-1}$. Note that the magnitude of $w_a^{\mathrm{inter}}$ appears to be even smaller than the spontaneous emission rate of a single molecule, which typically is of a few times $10^8\,\mathrm{s}^{-1}$. Certainly $w_a^{\mathrm{inter}}$ is much smaller than the spontaneous emission rate for an exciton state. It is to be noted furthermore that raising $N^*$ by a factor of 2 will reduce $w_a^{\mathrm{inter}}$ by almost two orders of magnitude. From the above, an important conclusion can be deduced: the intersegment channel of exciton–exciton annihilation is in fact ineffective at low temperatures, because the radiative relaxation is much faster. On the contrary, the intrasegment annihilation rate is fairly high and should be viewed as the unique way for two weakly localized excitons to annihilate at low temperature. However, since this process occurs only for doubly excited localization segments, it will affect the entire exciton population only if

the number of doubly excited segments is high, i.e., at sufficiently high laser intensities.

We note that the separation into intersegment and intrasegment annihilation channels was in fact concluded from transient absorption experiments on PIC *J*-aggregates at 20 K.[12,14] The part of the observed annihilation kinetics with a decay time of 200 fs may indeed be related to intrasegment annihilation, as is clear from our estimate for $w_a^{\mathrm{intra}}$. Our estimate for $w_a^{\mathrm{inter}}$ shows, however, that it is unlikely that the second component of the kinetics reported in Refs. 12 and 14, with a decay time of 1.5 ps, may indeed be ascribed to intersegment annihilation (see also the discussion in Refs. 18 and 19).

Our findings concerning the ineffectiveness of intersegment annihilation provide us with a way to control the exciton–exciton annihilation at low temperature. Indeed, recall that the local ground and first excited states belonging to the same localization segment are separated by the energy offset $E_2^*-E_1^*=3\pi^2U/(N^*+1)^2$, which is of the order of the *J*-band width.[20] For typical *J*-aggregates, the exciton radiative rate $\gamma$, representing the unique relaxation constant at low temperatures, is much smaller than this energy mismatch. Hence one may get a large number of localization segments to be singly excited by applying a field with Rabi frequency smaller than $E_2^*-E_1^*$, but larger than $\gamma$. At the same time, none of the localization segments will be doubly excited. Therefore, under such conditions, a fairly large exciton population may be created in *J*-aggregates, without being affected by exciton–exciton annihilation.

## ACKNOWLEDGMENTS

This work has been partially supported by INTAS (Project No. 97-10434). G.G.K. and V.A.M. also acknowledge support from the German Federal Ministry of Education, Science, Research, and Technology within the TRANSFORM—program (Project No. 01 BP 820/7). V.A.M. acknowledges the University of Juväskylä, where this work was started, for hospitality.

[1] G. J. Denton, N. Tessler, N. T. Harrison, and R. H. Friend, Phys. Rev. Lett. **78**, 733 (1997).
[2] H. Stiel, S. Daehne, and K. Teuchner, J. Lumin. **39**, 351 (1988).
[3] V. Sundström, T. Gillbro, R. A. Gadonas, and A. Piskarskas, J. Chem. Phys. **89**, 2754 (1988).
[4] M. van Burgel, D. A. Wiersma, and K. Duppen, J. Chem. Phys. **102**, 20 (1995).
[5] V. Sundström, in *J-Aggregates*, edited by T. Kobayashi (World Scientific, Singapore, 1996), p. 199.
[6] R. Gadonas, K.-H. Feller, A. Pugzlys, G. Jonusauskas, J. Oberlé, and C. Rulliere, J. Chem. Phys. **106**, 8374 (1997).
[7] L. Valkunas, G. Trinkunas, V. Liuolia, and R. van Grondelle, Biophys. J. **69**, 1117 (1995).
[8] S. de Boer and D. A. Wiersma, Chem. Phys. Lett. **165**, 45 (1990).
[9] H. Fidder, J. Knoester, and D. A. Wiersma, Chem. Phys. Lett. **171**, 529 (1990).
[10] H. Fidder, J. Terpstra, and D. A. Wiersma, J. Chem. Phys. **94**, 6895 (1991).
[11] H. Fidder, Ph.D. thesis, Groningen, 1993.
[12] K. Minoshima, M. Taiji, K. Misawa, and T. Kobayashi, Chem. Phys. Lett. **218**, 67 (1994).
[13] J. Moll, S. Daehne, J. R. Durrant, and D. A. Wiersma, J. Chem. Phys. **102**, 6362 (1995).
[14] T. Kobayashi and K. Misawa, in Ref. 5, p. 161.
[15] V. I. Bogdanov, E. N. Viktorova, S. V. Kulya, and A. S. Spiro, Pis'ma Zh. Eksp. Teor. Fiz. **53**, 100 (1991) [JETP Lett. **53**, 105 (1991)].
[16] Y. Wang, J. Opt. Soc. Am. B **8**, 981 (1991).
[17] S. Özçelik and D. L. Akins, J. Phys. Chem. B **101**, 3021 (1997).
[18] V. A. Malyshev, H. Glaeske, and K.-H. Feller, Chem. Phys. Lett. **305**, 117 (1999).
[19] V. A. Malyshev, H. Glaeske, and K.-H. Feller, Chem. Phys. **254**, 31 (2000).
[20] V. A. Malyshev, Opt. Spektrosk. **71**, 873 (1991) [Opt. Spectrosc. **71**, 505 (1991)]; J. Lumin. **55**, 225 (1993).
[21] V. Malyshev and P. Moreno, Phys. Rev. B **51**, 14587 (1995).
[22] M. Shimizu, S. Suto, T. Goto, A. Watanabe, and M. Matsuda, Phys. Rev. B **58**, 5032 (1998).
[23] V. A. Malyshev, A. Rodriguez, and F. Dominguez-Adame, Phys. Rev. B **60**, 14140 (1999).
[24] D. B. Chesnut and A. Suna, J. Chem. Phys. **39**, 146 (1963).
[25] Yu. A. Avetisyan, A. I. Zaitsev, and V. A. Malyshev, Opt. Spektrosk. **59**, 967 (1985) [Opt. Spectrosc. **59**, 582 (1985)].
[26] G. Juzeliunas, Z. Phys. D: At., Mol. Clusters **8**, 379 (1988).
[27] F. C. Spano, Phys. Rev. Lett. **67**, 3424 (1991); **68**, 2976(E) (1992).
[28] F. C. Spano and J. Knoester, in *Advances in Magnetic and Optical Resonance*, edited by W. S. Warren (Academic, New York, 1994), Vol. 18, p. 117.
[29] H. Fidder, J. Knoester, and D. A. Wiersma, J. Chem. Phys. **95**, 7880 (1991).
[30] L. D. Bakalis and J. Knoester, J. Phys. Chem. **103**, 6620 (1999); J. Lumin. **87-89**, 66 (2000).
[31] J. Knoester and F. C. Spano, Phys. Rev. Lett. **74**, 2780 (1995).
[32] T. T. Basiev, V. A. Malyshev, and A. K. Przhevuskii, in *Spectroscopy of Solids Containing Rare-Earth Ions*, edited by A. A. Kaplyanskii and R. M. MacFarlane (North-Holland, Amsterdam, 1987), p. 275.
[33] A. V. Malyshev and V. A. Malyshev (unpublished).
[34] P. O. J. Scherer, Adv. Mater. **7**, 451 (1995).